

## Electron paramagnetic resonance spectra of $\text{Er}^{3+}$ in the monoclinic $\text{KY}(\text{WO}_4)_2$ crystal

This article has been downloaded from IOPscience. Please scroll down to see the full text article.

2003 J. Phys.: Condens. Matter 15 5113

(<http://iopscience.iop.org/0953-8984/15/29/323>)

View [the table of contents for this issue](#), or go to the [journal homepage](#) for more

Download details:

IP Address: 171.66.16.121

The article was downloaded on 19/05/2010 at 14:20

Please note that [terms and conditions apply](#).

## Electron paramagnetic resonance spectra of $\text{Er}^{3+}$ in the monoclinic $\text{KY}(\text{WO}_4)_2$ crystal

M T Borowiec<sup>1,3</sup>, A A Prochorov<sup>2</sup>, A D Prochorov<sup>2</sup>, V P Dyakonov<sup>1,2</sup> and H Szymczak<sup>1</sup>

<sup>1</sup> Institute of Physics, al Lotników 32/46, 02-668 Warsaw, Poland

<sup>2</sup> A A Galkin Physico-Technical Institute, 72 R Luxemburg Street, 340114 Donetsk, Ukraine

E-mail: borow@ifpan.edu.pl

Received 4 April 2003, in final form 9 June 2003

Published 11 July 2003

Online at [stacks.iop.org/JPhysCM/15/5113](http://stacks.iop.org/JPhysCM/15/5113)

### Abstract

Electron paramagnetic resonance (EPR) studies of  $\text{Er}^{3+}$  of single-crystal  $\text{KY}(\text{WO}_4)_2$  have been carried out at X-band frequencies over a temperature range from 4.2 to 300 K. The main  $x$ - and  $z$ -axes of the  $g$ -tensor in the  $ac$  plane do not coincide with the crystallographic  $a$ - and  $c$ -axes, while the  $y$ - and  $b$ -axes are parallel. The EPR spectrum is characterized by a strong anisotropy of the  $g$ -factors ( $g_z = 13.25 \pm 0.05$ ,  $g_x = 0 \pm 0.1$ ,  $g_y = 3.378 \pm 0.005$ ) and of the hyperfine interaction parameters ( $A_z = -469 \pm 3$ ,  $A_x = 0 \pm 3.5$ ,  $A_y = -120.75 \pm 0.8$  in  $10^{-4} \text{ cm}^{-1}$ ). The temperature dependence of the  $g$ -factors is caused by an anharmonic part of the spin–phonon Hamiltonian as well as by a rotational contribution to this Hamiltonian. A spin–lattice relaxation is shown to result from two Orbach processes through the first and second excited levels of an electronic spectrum.

### 1. Introduction

Studies of rare-earth–alkali metal double tungstates are strongly stimulated by the possible application of these compounds as active materials for solid-state lasers. Optical spectra have been studied for most rare-earth ions in these crystals [1]. However, the ground-state characteristics of the rare-earth ions, which can be studied by using the technique of electron paramagnetic resonance (EPR), are not sufficiently well known. To date, the EPR spectra of only  $\text{Gd}^{3+}$  [2] and  $\text{Dy}^{3+}$  [3] ions have been investigated and the effects of low symmetry found. These manifest themselves in a different orientation of the  $g$ -tensor axes compared to the directions of the crystallographic axes. A mismatch was also observed in the angle of the axes of quantum transitions in the gadolinium spectrum. In EPR spectra of the  $\text{Dy}^{3+}$  ion, hyperfine interactions with the intrinsic nucleus and superhyperfine interactions with nuclei

<sup>3</sup> Author to whom any correspondence should be addressed.

of the tungstate have been observed. The latter are located outside the nearest dodecahedron of oxygen ions. Similar interactions were first determined in the spectrum from pairs of  $\text{Dy}^{3+}$  ions [4]. The paramagnetic ions in the crystals that were investigated are located in chains that are parallel to the crystallographic  $a$ -axis. This results in peculiarities of spin–spin interactions and the unusual EPR spectrum of dysprosium ions in the  $\text{KDy}(\text{WO}_4)_2$  single crystal [5]. The spectra of other rare-earth ions are expected to also possess interesting characteristics. In this paper the results of EPR studies on the  $\text{Er}^{3+}$  ions in the  $\text{KY}(\text{WO}_4)_2$  single crystal are presented.

## 2. Crystal structure and experiment

Crystals of rare-earth–alkali metal double tungstates  $\text{KA}(\text{WO}_4)_2$  (where  $A = \text{Y, Gd, } \dots, \text{Lu}$ ) belong to the centrosymmetric class of  $2/m$  monoclinic crystal system. The crystallographic structures of potassium–yttrium and isomorphous potassium–gadolinium double tungstates are described by the  $I2/c$  or  $C2/c$  space groups [6–10]. The lattice parameters of the unit cell for the  $I2/c$  and  $C2/c$  space groups are  $a = 8.05 \text{ \AA}$ ,  $b = 10.35 \text{ \AA}$ ,  $c = 7.54 \text{ \AA}$  and  $\beta = 94^\circ$  and  $a_1 = 10.64 \text{ \AA}$ ,  $b_1 = 10.35 \text{ \AA}$ ,  $c_1 = 7.54 \text{ \AA}$  and  $\beta = 130.5^\circ$ , respectively. The axes of transformations from the first to the second space group can be achieved through  $a_1 = a + c$ ,  $b_1 = b$  and  $c_1 = -c$ . The elementary cell with  $I2/c$  structure corresponds best to the habit of the crystal studied.

The yttrium and potassium ions occupy  $C2$  symmetry positions. Eight oxygen ions surrounding the  $\text{Y}^{3+}$  cations present polyhedra that are bonded to each other by their edges and constitute a continuous chain extended along the  $a$ -axis. The  $\text{K}^+$  cations are surrounded by 12 oxygen ions. The potassium–oxygen polyhedra present a distorted icosahedron forming chains along the  $a$ -axis. The tungstate ions, surrounded by six oxygen ions, form  $\text{WO}_4^{2-}$  octahedral anionic complexes. The  $\text{WO}_4$  octahedra constitute a double chain extended along the  $c$ -axis (for the  $C2/c$  space group).

The single crystals used in the EPR measurements were grown from a melt of potassium di-tungstate ( $\text{K}_2\text{W}_2\text{O}_7$ ) by a slow decrease in temperature from  $1050^\circ\text{C}$  at a rate of  $3^\circ\text{C h}^{-1}$ . Well faceted single crystals were produced, with a size of about 3 mm. The orientation of the crystals was established by x-ray diffraction.

To determine the main axes of the  $g$ -tensor using the EPR spectra, it should be necessary to fix the  $ac$  plane, because one of the main axes (the  $y$ -axis) is directed along the crystallographic  $b$ -axis (the  $C2$  axis) and other two main axes (the  $x$ - and  $z$ -axes) lie in the  $ac$  plane. The concentrations of  $\text{Er}^{3+}$  ions in the crystals studied were equal to 0.02 and 1%.

Measurements of EPR spectra were carried out using an X-band spectrometer with high-frequency modulation. The magnetic field was changed from 0 to 1 T. The sample temperature was varied in steps between 300 and 4.2 K by using a flowing helium gas cryostat.

## 3. Hyperfine structure and angular dependences of EPR spectra

The  $\text{Er}^{3+}$  ion has  $4f^{11}$  electronic configuration with the ground multiplet  $^4I_{15/2}$ . The low-symmetry crystal field splits this multiplet into eight Kramer's doublets. The EPR spectra were observed at the lowest doublet state of  $\text{Er}^{3+}$  ions. Figure 1 shows the EPR spectrum with a magnetic field oriented along the  $z$ -direction at a temperature of 4.2 K. It consists of the central intensive absorption line, which belongs to even isotopes of erbium, and eight lines of the hyperfine structure. The hyperfine structure is due to the interaction of electronic spin with nuclear magnetic moment (the nuclear spin of  $I = \frac{7}{2}$ ) of the odd isotope  $^{167}\text{Er}$  (the abundance

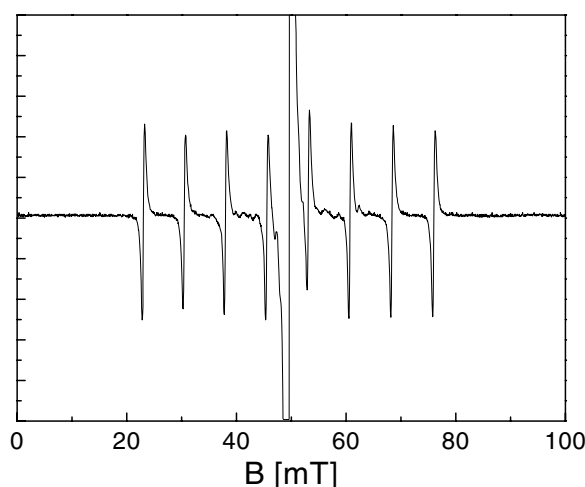


**Figure 1.** The EPR spectrum of the Er<sup>3+</sup> ion in KY(WO<sub>4</sub>)<sub>2</sub> with a magnetic field oriented along the *z*-direction at a temperature of 4.2 K.

**Table 1.** The values of the *g* and *A* parameters along the main axes of the *g*- and *A*-tensors.

Axis	<i>g</i>	<i>A</i> (10 <sup>-4</sup> cm <sup>-1</sup> )
<i>x</i>	0 ± 0.1	0 ± 3.5
<i>y</i>	3.378 ± 0.005	-120.75 ± 0.8
<i>z</i>	13.25 ± 0.05	-469 ± 3

of which is about 22.82%). The EPR spectrum is strongly anisotropic. Its behaviour in a magnetic field can be described by the spin-Hamiltonian with the effective spin  $S = \frac{1}{2}$ :

$$H = \beta SgB + SAI \quad (1)$$

where the first term describes the Zeeman splitting, the second term describes the hyperfine interaction with the erbium nucleus, *g* is the tensor of the spectroscopic splitting factor, and *A* is the tensor of the hyperfine interaction. The calculated spin-Hamiltonian parameters are presented in table 1.

It is seen that the maximal value of the *g*-tensor is *g<sub>z</sub>*. Figure 2 presents the angular dependence of the resonance field for an even isotope in the *ac(xz)* plane. The *z*-axis makes an angle of 54° with the *c*-axis and lies in the *ac* plane. Figure 3 presents the angular dependence of eight hyperfine structure lines in the *yz* plane near the *y*-axis. Such unusual angular dependences are associated with a strong anisotropy of the spin-Hamiltonian parameters. Similar angular dependence was observed in Er-doped lanthanum ethyl sulphate [11]. Because of the non-equidistance of lines near the *y*-axis, the sample orientation with respect to the magnetic field direction should be precise. The spin-Hamiltonian parameters were determined from the experimental angular dependence of the EPR line's position using a home-made diagonalization program of 16 × 16 matrices. The initial selection of *g*-factors using the even-isotope spectrum was performed via the standard expression

$$g^2 = g_z^2 \cos^2 \theta + g_x^2 \sin^2 \theta \cos^2 \phi + g_y^2 \sin^2 \theta \sin^2 \phi \quad (2)$$

where  $\theta$  and  $\phi$  are the polar and azimuthal angles describing the position of the external magnetic field.

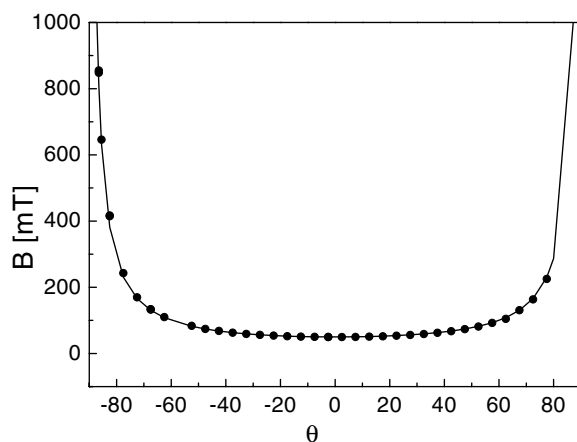


**Figure 2.** The angular dependence of the EPR line of the  $\text{Er}^{3+}$  even isotope in the  $yz$  plane. The angle  $\theta = 0$  corresponds to the  $z$ -direction.

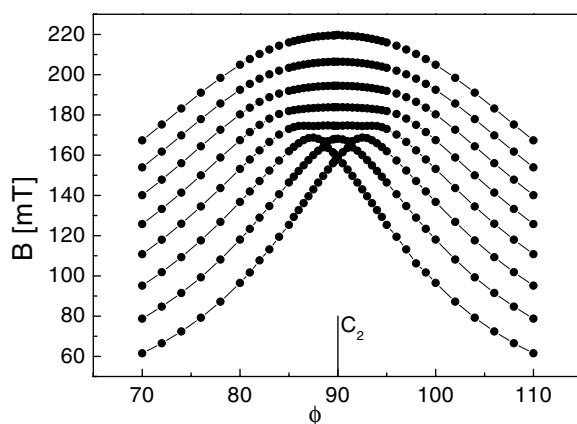


**Figure 3.** The angular dependence of the hyperfine structure lines of the  $\text{Er}^{3+}$  odd isotope near the  $C_2$  axis. The angle  $\theta = 90^\circ$  corresponds to the  $y$ -direction.

The angular dependences of the  $g$ - and  $A$ -tensors measured in the  $xz$  and  $yz$  planes have shown that the principal axes of the  $g$ - and  $A$ -tensors are practically the same. This implies that the low-symmetry crystalline field components that are characteristic of monoclinic symmetry are very small and do not cause an off-orientation of the axes of the hyperfine and Zeeman interactions.

In the crystal field approximation, and taking into account only the matrix elements between the states with a given value  $J$  (in our case,  $J = \frac{15}{2}$  for the  $^4I_{15/2}$  ground multiplet), the main values of the hyperfine splitting tensor  $A$  and of the  $g$ -tensor are connected as follow:

$$A_x/g_x = A_y/g_y = A_z/g_z = A_J/g_J \quad (3)$$

where  $g_J$  is the Landé factor and  $A_J$  is the constant of magnetic hyperfine interaction for the free  $\text{Er}^{3+}$  ion.

In our case, this ratio executes well:  $A_y^*g_z/A_z^*g_y = 1$ . This testifies that an admixture of higher-lying multiplets of the  $\text{Er}^{3+}$  ions is absent. Indeed, according to [12–14], the energy interval between the ground multiplet  $^4I_{15/2}$  and nearest excited multiplet  $^4I_{13/2}$  is equal to

6600 cm<sup>-1</sup>. The signs of the  $A_z$  and  $A_y$  tensors and the accuracy of finding  $A_x$  were also determined (table 1) using the above correlations and taking into account that  $A_J < 0$  [15].

The symmetry of the Er<sup>3+</sup> EPR spectra allow us to suppose that a doping ion can replace the Y<sup>3+</sup> ion in the KY(WO<sub>4</sub>)<sub>2</sub> lattice. The large difference between the ionic radii of K<sup>+</sup> (1.33 Å) and Er<sup>3+</sup> (0.89 Å) renders replacement of the K<sup>+</sup> site by the Er<sup>3+</sup> ion impossible (the ionic radius of Y<sup>3+</sup> is 0.92 Å). Additionally, in the case of the replacement of the K<sup>+</sup> site by the Er<sup>3+</sup> ion, it should be compensated by two excess charges. As a result, a non-equivalent EPR spectrum should appear. However, additional EPR lines in our experiment are not observed. These facts indicate that Er<sup>3+</sup> ions replace the Y<sup>3+</sup> ions only.

#### 4. Temperature dependence of the linewidth

The linewidth of EPR spectra ( $\Delta B$ , the peak-to-peak width of the absorption derivative) is anisotropic, namely  $\Delta B$  is equal to 0.37 and 1.96 mT for the  $z$ - and  $y$ -directions, respectively. Because of the small concentration of Er<sup>3+</sup> in the crystal, the linewidth cannot be due to the spin-spin interactions only and is induced rather by a distribution of the crystal field parameters due to lattice defects. The low-symmetry crystal field acting on the paramagnetic ion is responsible for the strong anisotropy of the  $g$ -factors. The angular dependence of the spectrum near the  $z$ -direction is weak, in contrast to its very strong dependence near the  $y$ -direction. The linewidth along the  $y$ -direction is larger than that along the  $z$ -direction by a factor of about four.

All rare-earth ions (except Gd<sup>3+</sup> with orbital momentum  $L = 0$ ) are strongly associated with lattice vibrations. Therefore, observation of EPR spectra is only possible at low temperatures. In our case, EPR was observed only at  $T < 40$  K. Above 40 K, the linewidth is so large that it is not possible to observe the EPR line. The EPR linewidth measurements were performed in the  $z$ - and  $y$ -directions. A spin-phonon contribution to the total linewidth ( $\Delta B_{sp}$ ) is calculated using the following formula:

$$\Delta B_{sp} = \Delta B - \Delta B_{4.2} \quad (4)$$

where  $\Delta B$  is the total linewidth and  $\Delta B_{4.2}$  is the linewidth at liquid helium temperature.

The temperature dependence of the spin-phonon part of the EPR linewidth is presented in figure 4. The solid curve represents the fitting of experimental data using two exponents. This indicates the occurrence of two exponential processes of spin-lattice relaxation through excited levels (the Orbach processes). Using the known formula [16]

$$T_1^{-1} = 1.4 \times 10^7 \pi g \Delta B_{sp} \quad (5)$$

where  $T_1$  is the spin-lattice relaxation time (in seconds), the relaxation time can be expressed as

$$T_1^{-1} = 1.1 \times 10^{10} \exp(-W_1/kT) + 5.74 \times 10^{11} \exp(-W_2/kT) \quad (6)$$

where  $W_1 = 36$  cm<sup>-1</sup> and  $W_2 = 84$  cm<sup>-1</sup> are the fitting parameters.

Spin-lattice relaxation is a complex phenomenon and can run through different processes, including the one-phonon and Raman two-phonon processes. However, in our case Orbach processes are predominant and run through the two doublet excited energy levels nearest to the ground state. The  $W_1$  and  $W_2$  values, obtained from analysis of the Er<sup>3+</sup> ion's optical spectra, are close to these. According to optical spectroscopy data [12–14], the multiplet <sup>4</sup> $I_{15/2}$  is split into eight Kramer's doublets with the following energy level positions: 0, 35, 77, 127, 169, 275, 343 and 361 cm<sup>-1</sup>. The  $W_1$  and  $W_2$  values are in satisfactory agreement with spectroscopy data, taking into account that the experimental error in determining the energy intervals between excited levels through the change in linewidth is about  $\pm 3$  cm<sup>-1</sup>.

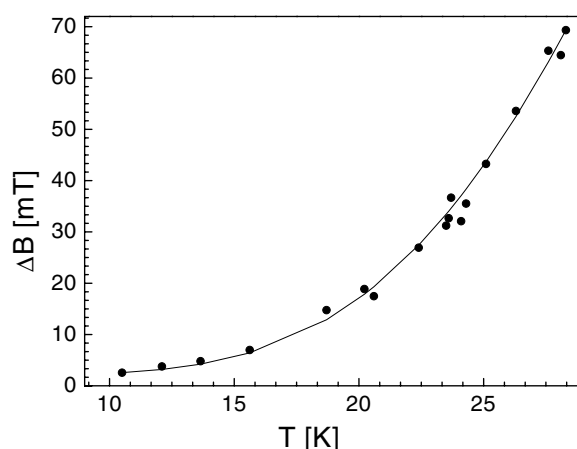


**Figure 4.** The temperature dependence of the EPR linewidth of even-isotope  $\text{Er}^{3+}$  along the  $y$ -direction ( $B \parallel C_2$ ).

### 5. Temperature dependence of the $g$ -factor

In parallel with the increase in EPR linewidth as the temperature is increased, the resonance fields are shifted towards higher fields in the  $z$ - and  $y$ -directions. This means that the  $g$ -factor decreases. This phenomenon was first observed in the EPR spectra of the  $\text{Dy}^{3+}$  ion [3]. Figure 5 presents the temperature dependences of the  $g_z$ - and  $g_y$ -factors, which are nonlinear functions of temperature. To date, the temperature dependences of both the  $g$ -factors and the hyperfine interactions for ions with frozen orbital momentum have been studied. In this case, the interaction of ions with lattice vibrations are ineffective and the EPR spectra and their dependence on temperature could be observed at room temperature and above. Unlike the Fe group of ions, the spin-orbit interaction value for rare-earth ions is high. As a result, rare-earth ions (except those with half-filled shells) interact strongly with lattice vibrations and are characterized by a short spin-lattice relaxation time, while the EPR spectra are usually not observable at temperatures higher than 30–40 K. The theory of the temperature dependence of the spin-Hamiltonian parameters (including the hyperfine interactions) was developed in [17, 18]. It has been shown that this effect is related to the dynamic spin-Hamiltonian, which should be rotationally invariant. Generally, the temperature dependence of the spin-Hamiltonian parameters arises due to an anharmonic part of the spin-phonon Hamiltonian as well as the rotational contribution to the dynamic spin-Hamiltonian. Within the frame of the model that has been developed, the temperature dependence of the  $g$ -factor arises, assuming that the spin-phonon interaction is described by the following Hamiltonian:

$$H_{\text{sp}} = \sum_{ijkl} F_{ijkl} S_i H_j E_{kl} \quad (7)$$

where  $F_{ijkl}$  is the magnetoelastic tensor and  $E_{kl}$  is the finite strain tensor.

In the Debye model, the temperature dependence of the  $g$ -factor is proportional to [17, 18]

$$T^4 \int_0^{\theta/T} \frac{x^3 dx}{e^x - 1} \quad (8)$$

where  $x = h\nu/kT$ ,  $h$  is the Planck constant,  $\nu$  is the phonon frequency,  $k$  is the Boltzmann constant, and  $\theta$  is the Debye temperature. Since the  $\theta$  temperature in the crystals studied is high (about 280 K) [19], the factor of  $T^4$  is practically temperature independent in the temperature

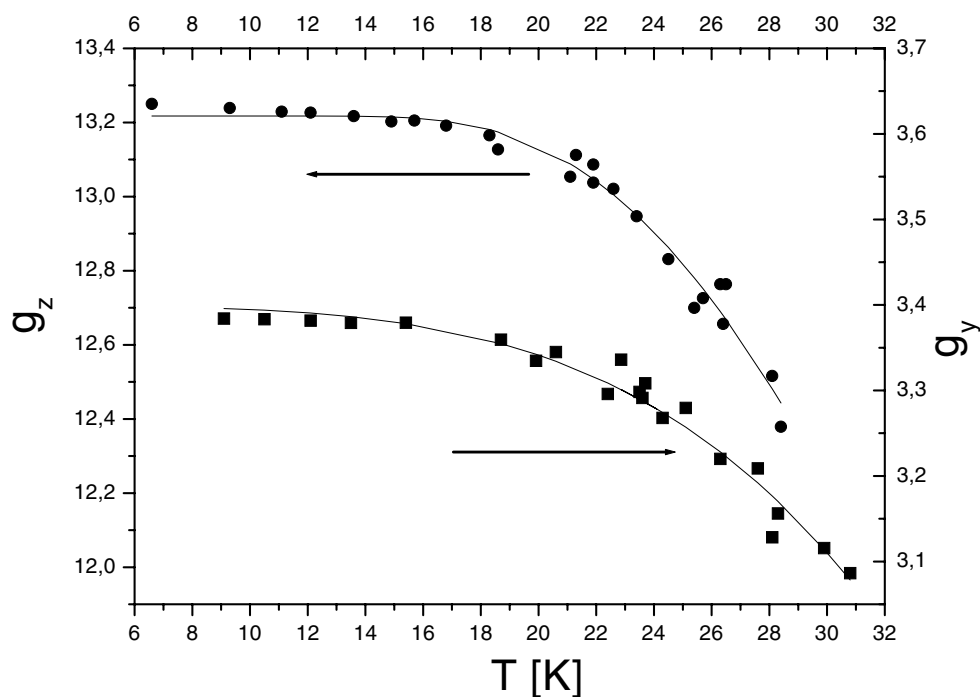


**Figure 5.** The temperature dependence of the  $g_z$ - and  $g_y$ -factors. The points are experimental data and the solid line represents the theoretical curve, according to equation (8).

region investigated (i.e. below 30 K). The excited states of the rare-earth ion give a negligible contribution to the temperature shift of the EPR line. In figure 5, the solid lines present the fitting curve proportional to  $T^4$ . One can see that the calculated curves are in good agreement with the experimentally observed temperature dependences of the  $g$ -factor.

## 6. Conclusions

The EPR spectrum of the  $\text{Er}^{3+}$  ion that partially substitutes the diamagnetic  $\text{Y}^{3+}$  ion in  $\text{KY}(\text{WO}_4)_2$  is found to be strongly anisotropic. The values of both the  $g$ -tensor and the hyperfine interaction parameters along different crystallographic axes differ strongly. The strong anisotropy is responsible for both the ‘wave’ angular dependence of the hyperfine structure near to the  $C2$  axis and the non-equidistance of the hyperfine lines for this orientation.

The spin–phonon broadening of the EPR line with increasing temperature is associated with relaxation processes (namely Orbach processes) through the two doublet excited states nearest to the ground state. The energy levels determined using the temperature dependence of the EPR linewidth are close to the data obtained from optical spectroscopy.

The main  $x$ - and  $z$ -axes of the  $g$ -tensor in the  $ac$  plane were determined. Their directions do not coincide with the crystallographic  $a$ - and  $c$ -axes, respectively, and differ from the analogous directions of the  $x$ - and  $z$ -axes for the  $\text{Dy}^{3+}$  ion [3]. For the  $\text{Er}^{3+}$  ion, the angles between the magnetic and crystallographic axes are larger than those for the  $\text{Dy}^{3+}$  ion [3].

The temperature dependence of the  $g$ -factors is caused by an anharmonic part of the spin–phonon Hamiltonian as well as by the rotational contribution to this Hamiltonian. A spin–lattice relaxation is shown to result from two Orbach processes through the first and second excited levels of an electronic spectrum.

## Acknowledgments

The authors are grateful to G Ya Samsonova and L F Chernykh for the growth of the single crystals and T Zayarniuk for technical support. This work is supported in part by the Polish Committee on Science (KBN), project no 2P03B 141 18.

## References

- [1] Kaminskii A A, Konstantinova A F, Orekhova V P, Butashin A V, Klevtsova R F and Pavlyuk A A 2001 *Crystallography* **46** 733
- [2] Borowiec M T, Dyakonov V, Kamenev V, Krygin I, Piechota S, Prokhorov A and Szymczak H 1998 *Phys. Status Solidi b* **209** 443
- [3] Borowiec M T, Dyakonov V, Prokhorov A and Szymczak H 2000 *Phys. Rev. B* **62** 5834
- [4] Krygin I, Prokhorov A, Dyakonov V, Borowiec M T and Szymczak H 2002 *Phys. Solid State* **44** 1513 (in Russian)
- [5] Borowiec M T, Dyakonov V P, Prokhorov A D and Szymczak H 1997 *Physica B* **240** 21
- [6] Klevtsov P V, Kozeeva L P and Klevtsova R F 1968 *Izv. Akad. Nauk SSSR Neorg. Mater.* **4** 1147 (in Russian)
- [7] Borisov S V and Klevtsova R F 1968 *Crystallography* **13** 517
- [8] Viscakas J K, Mochalov I V, Mikhailov A V, Klevtsova R F and Lyubimov A V 1988 *Litov. Fiz. Sb.* **28** 224
- [9] Zaldo C, Rico M, Cascales C, Pujol M C, Massons J, Aguilo M, Diaz F and Porcher P 2000 *J. Phys.: Condens. Matter* **12** 8531
- [10] Macalik L, Hanuza J, Macalik B, Ryba-Romanowski W, Golab S and Pietraszko A 1998 *J. Lumin.* **79** 9
- [11] Barzii I V, Neilo G N and Prokhorov A D 1993 *Fiz. Tekh. Vysokikh Davlenii* **3** 23 (in Russian)
- [12] Pujol M C, Rico M, Zaldo C, Sole R, Nikolov V, Solans X, Aguilo M and Diaz F 1999 *Appl. Phys. B* **68** 187
- [13] Kaminskii A A, Pavlyuk A A, Butaeva T I, Fedorov V A, Balashov I F, Berenberg V A and Lyubchenko V V 1977 *Izv. Akad. Nauk SSSR Neorg. Mater.* **13** 1541 (in Russian)
- [14] Malkin B Z, Kaminskii A A, Agamalyan N R, Bumagina L A and Butaeva T I 1982 *Phys. Status Solidi b* **110** 417
- [15] Abraham A and Bleaney B 1970 *Electronic Paramagnetic Resonance of Transition Ions* (Oxford: Clarendon)
- [16] Antipin A A, Katyshev A N, Kurkin I N and Shekun L Ya 1967 *Phys. Solid State* **9** 813 (in Russian)
- [17] Bates C A and Szymczak H 1976 *Phys. Status Solidi b* **74** 225
- [18] Bates C A and Szymczak H 1977 *Z. Phys. B* **28** 67
- [19] Szewczyk A, Gutowska M U, Piotrowski K, Gutowski M, Borowiec M T, Dyakonov V P, Kovarskii V L, Szymczak H and Gladczuk L 1998 *J. Phys.: Condens. Matter* **10** 10539